ISSN: 2302-9285, DOI: 10.11591/eei.v13i4.7270

# Robust hybrid control strategy for active power management in Kabertene wind farm within Algeria's PIAT grid

Tadjeddine Ali Abderrazak<sup>1</sup>, Arbaoui Iliace<sup>2</sup>, Hamiani Hichem<sup>1</sup>, Bendelhoum Mohamed Sofiane<sup>1</sup>, Bendeillali Ridha Ilyas<sup>1</sup>

<sup>1</sup>LSETER Laboratory, Department of Electrical Engineering, Technology Institute, Nour Bachir University Center, El-Bayadh, Algeria <sup>2</sup>Department of Material Sciences, Faculty of Material Sciences, Mathematics, and Computer Science, University Ahmed Draia, Adrar, Algeria

#### **Article Info**

## Article history:

Received Jul 29, 2023 Revised Aug 30, 2023 Accepted Oct 3, 2023

#### Keywords:

Doubly fed induction generator Passivity-based control Pole insalah-adrar-timimoune grid stability Renewable energy sources integration Simultaneous interconnection and damping assignment Wind turbine

#### **ABSTRACT**

The paper introduces a hybrid control strategy for optimised active power management in Algeria's Kabertene wind farm, crucial for the pole insalahadrar-timimoune (PIAT) grid's stability. This strategy merges simultaneous interconnection and damping assignment (SIDA) passivity theory, passivitybased control (PBC), and multivariable proportional-integral-derivative (PID) controllers. This combined approach ensures frequency and voltage stability within the PIAT grid, which encompasses various elements like wind farms, solar plants, gas turbines, and dynamic impedance (Z), current (I), and active power (P) (D-ZIP), load model. By tailoring controllers for doubly fed induction generators (DFIGs) using SIDA-PBC principles and optimising internal parameters, the strategy achieves precise control of active power output. Additionally, particle swarm optimisation (PSO) refines power scheduling, which is especially beneficial for intermittent renewable sources like DFIGs. This comprehensive strategy offers numerous advantages: improved network stability, minimized voltage deviations, reduced frequency fluctuations, and enhanced integration of renewable sources. The paper emphasises practical implementation considerations, providing valuable guidance for efficient Kabertene wind farm operation and integration. This research contributes significantly to fostering cleaner and more reliable energy systems, facilitating the PIAT grid's transition towards sustainable energy generation.

This is an open access article under the CC BY-SA license.



2202

#### Corresponding Author:

Tadjeddine Ali Abderrazak Department of Electrical Engineering, Technology Institute, University Center Nour Bachir El-Bayadh, Algeria Email: atadj1@gmail.com

#### 1. INTRODUCTION

The ecosystem has been irreparably damaged by the historical preponderance of fossil fuels in global energy production; this is evidenced by climate change, air and water pollution, and biodiversity loss [1]. With the increasing severity of these environmental issues, the adoption of renewable energy sources is no longer merely a choice, but an imperative. Integration of variable renewable energy (VRE) sources, such as wind and solar power, into extant electricity grids [2], [3] is a critical component of this transition. Nevertheless, the sporadic characteristics of VRE generation pose a unique array of obstacles. By storing excess energy during periods of high generation and releasing it during periods of low generation, energy storage systems have become an indispensable technology for managing this intermittency and assuring grid stability by maintaining a constant balance between supply and demand.

Journal homepage: http://beei.org

For this energy transition, the pole insalah-adrar-timimoune (PIAT) power network in southern Algeria is an illustrative case study. PIAT operates autonomously from the national infrastructure, utilising renewable electricity generated locally, predominantly from wind and solar sources (as illustrated in Figure 1) [4]. Regarding the 153 GWh of annual energy demand anticipated in 2023, VRE sources are anticipated to provide 18.67% [5]. The considerable dependence on renewable energy sources possesses the capacity to generate noteworthy ecological advantages, such as diminished carbon emissions [6], fortified environmental safeguarding, and enhanced energy accessibility for nearby communities [7]–[9].

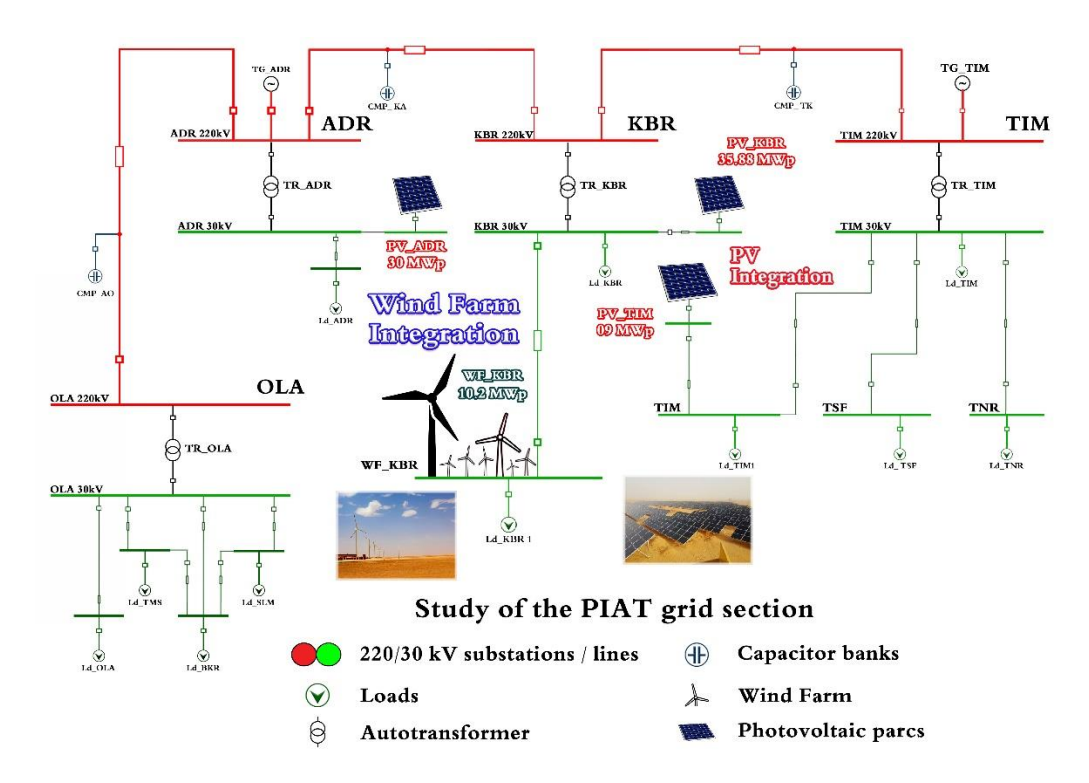


Figure 1. The PIAT electrical grid section study: Kabertene photovoltaic (PV) and wind farms

Algeria's progress towards establishing an energy infrastructure that is more ecologically sustainable is exemplified by the PIAT network [10], [11]. This network takes advantage of the country's indigenous renewable resources to tackle urgent environmental issues. This case study highlights the potential of renewable energy to promote environmental preservation and ensure equitable access to energy, in addition to mitigating climate change.

Wind turbines are of utmost importance in the realm of renewable energy owing to their negligible ecological footprint. However, these systems are accompanied by intricacies, such as dynamic power consumption patterns and non-linear load models [12], [13]. The comprehension and representation of these behaviours are fundamental in the field of grid management. Wind turbines, (doubly fed induction generators (DFIGs) in particular), are susceptible to grid malfunctions as a result of their direct stator-grid connection [14]. For turbine safety and stability, robust control strategies are crucial [15], particularly in locations such as the Kabertene PV and Wind Parks in Algeria as illustrated in Figure 1.

Due to their susceptibility to rotor winding problems brought about by overvoltage and overcurrent, which are predominantly induced by negative sequence voltage, DFIG systems present a unique challenge. The adverse sequence voltage has the potential to induce rotor slip, thereby causing detrimental overvoltage and overcurrent in the winding. Such conditions can compromise the turbine's dependability and effectiveness. Notwithstanding these obstacles, DFIGs present numerous benefits as prevalent varieties of wind turbines, such as the ability to operate at variable speeds and efficient power conversion [16], [17].

Despite this, stability concerns may arise during transient events due to the complexity of their components, including the rotor, stator, slip rings, and alternating current-direct current (AC-DC)-AC conversion [18]. Passive control methods for managing active and reactive power production, integration, and power flow analysis in DFIG systems are the primary focus of our research. We evaluated the efficacy of these control strategies by implementing them on the 10.2 MW Kabertene wind farm, which is connected to

2204 □ ISSN: 2302-9285

Algeria's PIAT grid. The outcomes of our study demonstrate that the control strategy we have suggested modulates the power outputs of DFIGs [19], [20].

In addition, grid stability is improved with the incorporation of a, especially in the face of disturbances [21], [22]. As the PIAT grid increasingly incorporates renewable energy sources such as wind and solar, frequency regulation becomes even more crucial. With average wind velocities ranging from 3 to 5 metres per second as showed in Figure 2, the region has a significant wind energy potential; this emphasises the need for effective control strategies [23].

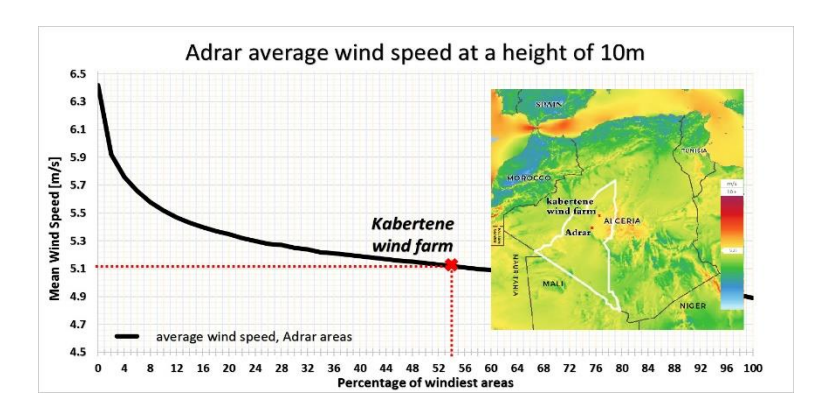


Figure 2. The mean wind speed at 10 m in kabertene and Adrar region, Algeria

Grid stability relies on frequency management, which is crucial for variable renewable energy (VRE) systems [24]. Insufficient production of renewable energy can lead to decreases in frequency, while excessive production can generate increases in frequency. It is crucial to maintain this balance in order to guarantee the stability of the power system [25]. Figure 3 illustrates the block design of the wind DFIG construction, which incorporates maximum power point tracking (MPPT), interconnection and damping assignment passivity-based control (IDA-PBC), and SIDA-PBC [26], [27].

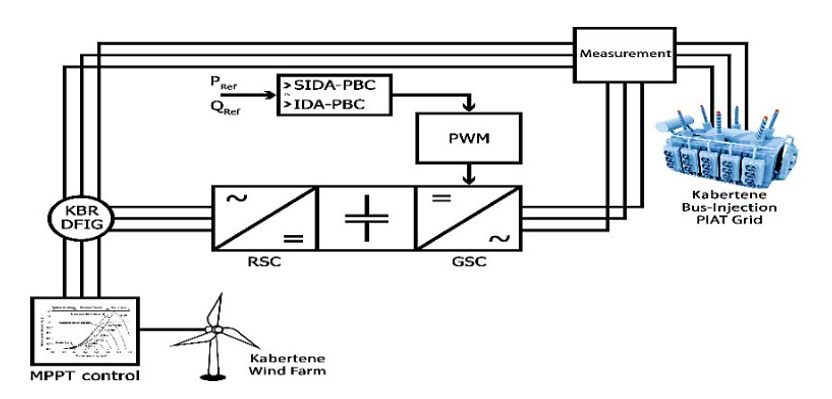


Figure 3. Block diagram of wind DFIG structure with MPPT, SIDA-PBC, and IDA-PBC control

The work we have conducted makes important contributions to the comprehension of control system design for DFIGs in wind farms. The proposed inner-droop control technique with SIDA-PBC has multiple benefits, such as increased resistance to wind speed variations and improved responsiveness to sudden changes [28]. Moreover, Figure 4 illustrates the progression of the daily load profile for PQ buses, highlighting the distinct patterns of electricity consumption during peak and off-peak periods [29]. There is a rise in demand between the morning and evening, which aligns with times of intense residential and commercial activity. This is evident from the swings observed on weekdays [30].

Our study offers a comprehensive understanding of the challenges and control strategies in wind energy, specifically within the Kabertene wind farm in the PIAT grid. It underscores the potential of renewable energy sources to shape a sustainable and eco-friendly energy landscape [31]. By addressing VRE integration complexities, grid stability, and control strategies, we contribute to the ongoing shift towards cleaner and more reliable energy systems, advancing the path to a sustainable energy future [32].

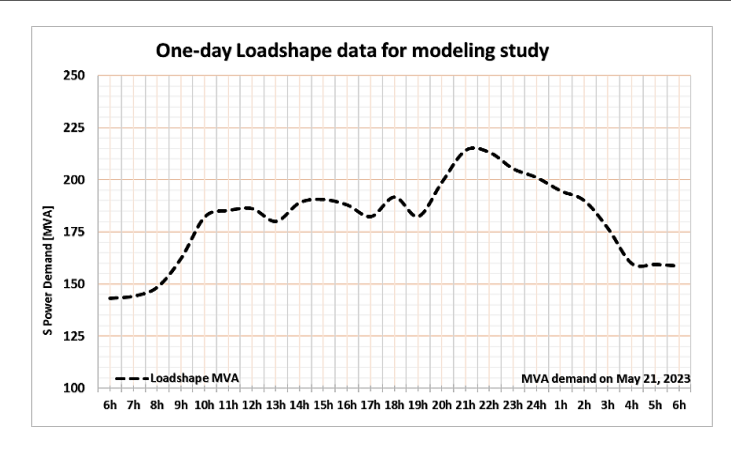


Figure 4. Evolution of the daily load profile in grid study

# 2. MATERIALS AND FORMULATION

#### 2.1. Wind turbine port-controlled hamiltonian modeling

The paper delves into a comprehensive analysis of control for DFIGs in wind energy systems, emphasizing the critical role of stability in wind farm reliability. The paper introduces various mathematical equations and models to describe the behavior and control of DFIGs in wind turbines. Key equations and concepts presented in the paper are summarized:

ZIP model (1): describes the general form of the ZIP (impedance-current-active power) model, commonly
used in power system analysis. It characterizes power consumption as a function of voltage and frequency.

$$\begin{cases} P = P_0 \left[ a_p \left( \frac{v}{v_o} \right)^2 + b_p \left( \frac{v}{v_o} \right) + c_p \right] \left[ 1 - k_{pf} \Delta f \right] \\ Q = Q_0 \left[ a_q \left( \frac{v}{v_o} \right)^2 + b_q \left( \frac{v}{v_o} \right) + c_q \right] \left[ 1 - k_{qf} \Delta f \right] \end{cases}$$

$$(1)$$

Wind power (2): defines wind power generation as a function of wind speed.

$$P_{v} = \frac{1}{2}\sigma.S.v^{3} \tag{2}$$

 Aerodynamic power (3): describes the aerodynamic power of a wind turbine, which depends on the coefficient of aerodynamic power (Cp) and environmental factors like air density and wind speed.

$$P_{aero} = C_p \cdot P_v = C_p(\lambda, \beta) \frac{1}{2} \rho \cdot S \cdot v^3$$
(3)

- Coefficient of aerodynamic power (4): provides a formula for Cp, considering factors such as tip-speed ratio ( $\lambda$ ) and blade pitch angle ( $\beta$ ).

$$C_p(\lambda, \beta) = C_1 \left( C_2 \frac{1}{\lambda} - C_3 \beta^x - C_4 - C_5 \right) e^{-\left(\frac{1}{\lambda + 0.08\beta} - \frac{0.035}{1 + \beta^3}\right)} C_6 \tag{4}$$

 Torque and mechanical speed (5)-(8): describe the relationship between torque, mechanical power, and mechanical speed in a wind turbine.

$$T_{mec} = \frac{P_{mec}}{w} = \frac{1}{2} \frac{\rho \cdot S \cdot v^3 C_p(\lambda, \beta)}{w} \tag{5}$$

$$J\frac{d\Omega_{mec}}{dt} = T_{mec} \tag{6}$$

$$J = \frac{J_{turbine}}{G} + J_{DFIG} \tag{7}$$

$$T_{mec} = T_a - T_{em} - T_{vis} \tag{8}$$

 DFIG PCH model (9): presents the model of a in the d-q reference frame, considering voltage and current components.

$$\begin{cases} V_{ds} = R_s I_{ds} + \frac{d\Phi_{ds}}{dt} - \omega_s \Phi_{qs} \\ V_{qs} = R_s I_{qs} + \frac{d\Phi_{qs}}{dt} + \omega_s \Phi_{ds} \\ V_{dr} = R_r I_{dr} + \frac{d\Phi_{dr}}{dt} - (\omega_s - \omega) \Phi_{qr} \\ V_{qr} = R_r I_{qr} + \frac{d\Phi_{qr}}{dt} + (\omega_s - \omega) \Phi_{dr} \\ J_{\frac{d\omega}{dt}} = M (I_{dr} I_{qs} - I_{ds} I_{qr}) - C_r - C_f \omega \end{cases}$$

$$(9)$$

- Equations of flux linkages (10)-(12): describes the dynamics of flux linkages in the DFIG model.

$$\begin{cases} \dot{\Phi}_{ds} = V_{ds} - R_{s}I_{ds} + \omega_{s}L_{s}I_{qs} + \omega_{s}MI_{qr} \\ \dot{\Phi}_{qs} = V_{qs} - R_{s}I_{qs} - \omega_{s}L_{s}I_{ds} - \omega_{s}MI_{dr} \\ \dot{\Phi}_{dr} = V_{dr} - R_{r}I_{dr} + (\omega_{s} - \omega)L_{r}I_{qr} + (\omega_{s} - \omega)MI_{qs} \\ \dot{\Phi}_{qr} = V_{qr} - R_{r}I_{qr} - (\omega_{s} - \omega)L_{r}I_{dr} - (\omega_{s} - \omega)MI_{ds} \end{cases}$$
(10)

$$\begin{cases} \dot{\Phi}_{s} = V_{s} - R_{s} I_{2} I_{s} - \omega_{s} L_{s} J_{2} I_{s} - \omega_{s} M J_{2} I_{r} \\ \dot{\Phi}_{r} = V_{r} - R_{r} I_{2} I_{r} - (\omega_{s} - \omega) M J_{2} I_{s} - (\omega_{s} - \omega) L_{r} J_{2} I_{r} \\ J_{DFIG} \frac{d\omega}{dt} = L_{sr} I_{s}^{T} J_{2} I_{r} - C_{r} - C_{f} \omega \end{cases}$$
(11)

$$\mathbf{x} = \left[\Phi_{\mathbf{s}}^{\mathsf{T}}, \Phi_{\mathbf{r}}^{\mathsf{T}}, \mathsf{J}_{\mathsf{DFIG}}\omega\right]^{\mathsf{T}} = \left[x_{\mathbf{e}}^{\mathsf{T}}, \mathsf{x}_{\mathsf{m}}\right]^{\mathsf{T}} \tag{12}$$

- Energy function (13) and (14): defines the energy function for the DFIG system, considering both electrical and mechanical components.

$$H(x) = \frac{1}{2} x_e^T L^{-1} x_e + \frac{1}{2 \log G} x_m^2$$
 (13)

$$\text{With:} \Phi_s = \begin{bmatrix} \Phi_{ds} \\ \Phi_{qs} \end{bmatrix}, \Phi_r = \begin{bmatrix} \Phi_{dr} \\ \Phi_{qr} \end{bmatrix}, I_s = \begin{bmatrix} I_{ds} \\ I_{qs} \end{bmatrix}, I_r = \begin{bmatrix} I_{dr} \\ I_{qr} \end{bmatrix}, I_2 = \begin{bmatrix} 1 & 0 \\ 0 & 1 \end{bmatrix}, J_2 = \begin{bmatrix} 0 & -1 \\ 1 & 0 \end{bmatrix}, L = \begin{bmatrix} L_s I_2 & M I_2 \\ M I_2 & L_r I_2 \end{bmatrix}$$

The partially differentiated of energy given by:

$$\begin{cases} \frac{\partial H}{\partial x_{e}} = L^{-1}x_{e} \\ \frac{\partial H}{\partial x_{m}} = J_{DFIG}^{-1}x_{m} \end{cases} \Longrightarrow \begin{cases} \frac{\partial H}{\partial x_{e}} = L^{-1}x_{e} = I = [I_{s}^{T}, I_{r}^{T}]^{T} \\ \frac{\partial H}{\partial x_{m}} = J_{DFIG}^{-1}x_{m} = \omega \end{cases}$$
(14)

 Interconnection and depreciation matrices (15) and (16): introduces matrices for system interconnection and depreciation.

$$\begin{cases}
J(\mathbf{x}) = \begin{bmatrix} -\omega_{s} L_{s} J_{2} & -\omega_{s} M J_{2} & 0_{2\times 1} \\ -\omega_{s} L_{s} J_{2} & -(\omega_{s} - \omega) L_{s} J_{2} & M J_{2} I_{s} \\ 0_{1\times 2} & M I_{s}^{T} J_{2} & 0 \end{bmatrix} \\
R(\mathbf{x}) = \begin{bmatrix} R_{s} I_{2} & 0_{2\times 2} & 0_{2\times 1} \\ 0_{2\times 2} & R_{r} I_{2} & 0_{2\times 1} \\ 0_{1\times 2} & 0_{1\times 2} & C_{f} \end{bmatrix}
\end{cases} (15)$$

With:  $g(x) = \begin{bmatrix} I_2 & O_{2\times 2} & O_{2\times 1} \\ O_{2\times 2} & I_2 & O_{2\times 1} \\ O_{1\times 2} & O_{1\times 2} & 1 \end{bmatrix}$ ,  $u = [V_s^T & V_r^T & T_r]^T$ 

Finally, the interconnection, depreciation and control matrices are:

$$\begin{cases} \dot{x} = \begin{bmatrix} -\omega_{s}L_{s}J_{2} & -\omega_{s}MJ_{2} & 0_{2\times1} \\ -\omega_{s}MJ_{2} & -(\omega_{s}-\omega)L_{s}J_{2} & MJ_{2}I_{s} \\ 0_{1\times2} & MI_{s}^{T}J_{2} & 0 \end{bmatrix} - \begin{bmatrix} R_{s}I_{2} & 0_{2\times2} & 0_{2\times1} \\ 0_{2\times2} & R_{r}I_{2} & 0_{2\times1} \\ 0_{1\times2} & 0_{1\times2} & T_{f} \end{bmatrix} \nabla H + \begin{bmatrix} I_{2} & 0_{2\times2} & 0_{2\times1} \\ 0_{2\times2} & I_{2} & 0_{2\times1} \\ 0_{1\times2} & 0_{1\times2} & 1 \end{bmatrix} \begin{bmatrix} V_{s}^{T} \\ V_{r}^{T} \\ T_{r} \end{bmatrix} \\ \dot{y} = \begin{bmatrix} I_{2} & 0_{2\times2} & 0_{2\times1} \\ 0_{2\times2} & I_{2} & 0_{2\times1} \\ 0_{1\times2} & 0_{1\times2} & 1 \end{bmatrix} \nabla H \end{cases}$$
 (16)

 SIDA passivity-based control (17): outlines the SIDA-PBC design for wind system modeling, focusing on matrix solutions and energy functions.

$$[J(I_s, \omega) - R]\partial H + \begin{bmatrix} V_s \\ 0_{2\times 1} \\ C_{em} \end{bmatrix} + \begin{bmatrix} 0_{2\times 2} \\ I_2 \\ 0_{1\times 2} \end{bmatrix} V_r = F_d(x)P_d\tilde{x}$$
(17)

 Control voltages (18): provides expressions for the control voltages of the DFIG in closed-loop systems, considering various parameters like damping and mechanical speed.

$$V_r = R_r I_r + (\omega_s - \omega) J_2 (M I_s + L_r I_r) - K_s (L_s \tilde{I}_s + M \tilde{I}_r) - K_r (L_r \tilde{I}_r + M \tilde{I}_s) + K_\omega J_2 \Phi_s \widetilde{\omega}$$
 (18)

With: 
$$K_r > 0$$
,  $K_\omega = \frac{P_\omega J_{DFIGM}}{P_{r\mu}} > 0$  et  $K_s > \frac{M^2}{4C_f L_r L_r \mu} |\Phi_r^*|^2 K_\omega$ .

- Closed-loop system (19): describes the dynamics of the closed-loop system, incorporating controller matrices.

$$f(x) + g(x)u = (J_d(x) - R_d(x))\partial H_d(x)$$
(19)

Where: 
$$\begin{cases} J_{a}(x) = J(x) + J_{a}(x) \\ R_{d}(x) = R(x) + R_{a}(x) \\ H_{d}(x) = H(x) + H_{a}(x) \end{cases}$$

 Command voltages (20)-(22): presents equations for the rotor voltages of the DFIG, including the effects of controller actions and mechanical speed.

$$J_{rm}(x) = MJ_2I_s \tag{20}$$

The closed-loop dynamic system is always of the form (19) with:

$$J_d(x) = \begin{bmatrix} -\omega_s L_s J_2 & -\omega_s M J_2 & 0_{2\times 1} \\ -\omega_s M J_2 & -\omega_r L_s J_2 & M J_2 I_s \\ 0_{1\times 2} & M I_s^T J_2 & 0 \end{bmatrix}; R_d(x) = \begin{bmatrix} R_s I_2 & 0_{2\times 2} & 0_{2\times 1} \\ 0_{2\times 2} & (R_r + r) I_2 & 0_{2\times 1} \\ 0_{1\times 2} & 0_{1\times 2} & T_f + \xi(x) \end{bmatrix}$$
(21)

Finally, the rotor voltages of the order are written by:

$$\begin{cases} V_r = V_r^* - (\omega - \omega^*)(L_r J_2 I_r^* + M J_2 I_s) - M \omega^* J_2 (I_s - I_s^*) - r I_2 (I_r - I_r^*) \\ V_r^* = (\omega_s - \omega^*)(L_r J_2 I_r^* + M J_2 I_s) + R_r I_2 I_r^* \end{cases}$$
(22)

The paper's mathematical framework and models contribute to the understanding and control of DFIGs in wind energy systems, ensuring stable and reliable performance.

## 3. RESULTS AND DISCUSSION

The simulation results were analyzed and represented using the stability analysis of small signals, dynamic voltage, and resolution with PSO algorithms method. The study was conducted on the 220 KV and the 60 KV on of the electrical PIAT grid region in southen Algeria (Figure 1). The software used for the analysis and representation of the results were MATLAB 2021a and ETAP 2019.

## 3.1. Frequency and voltage grid result

Figures 5(a) to (c) displays the evolution of the synchronism frequency correction  $f_r$  at the integration point of Kabertene (bus 4) alongside the frequency prediction model  $f_p$ . Figure 6 presents a depiction of the highest voltage levels registered at both the 220 KV transmission and 30 KV distribution buses. This representation takes into account the deployment of frequency control methodologies under two scenarios: one involving PV sources integrated with MPPT for PV production, and the other without PV sources. The graph specifically illustrates the pinnacle voltage values recorded throughout the operational phases of the electrical system.

2208 ☐ ISSN: 2302-9285

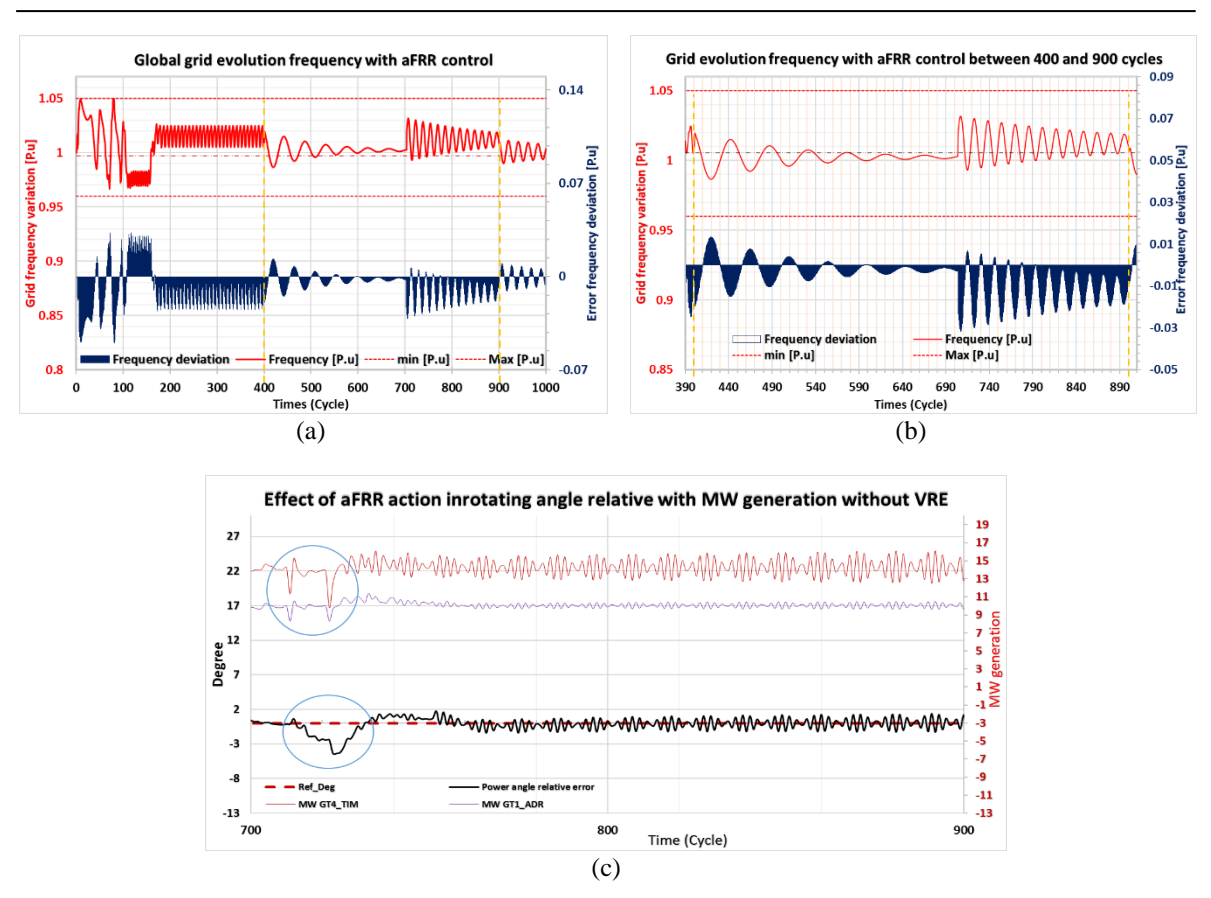


Figure 5. Evolution of the network frequency with correction of the automatic frequency restoration reserve (aFRR): (a) global control with 1000 cycles, (b) control zoom between 400 and 900 cycles, and (c) the effect of the aFRR action in relative rotation angle with MW generation without VRE

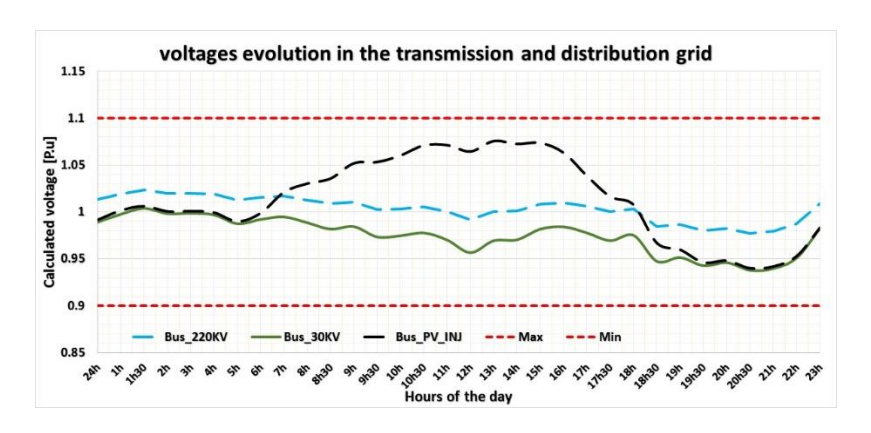


Figure 6. Voltages evolution in the 220 KV transmission and 30 KV distribution with PV injection bus

## 3.2. Doubly fed induction generator results

In order to assess the robustness of the DFIG, it is common practice to modify the internal resistance parameter and then observe the responses of the control approaches being used. It is necessary to carefully examine important parameters such as stability, transient responsiveness, power efficiency, and other relevant performance benchmarks.

Examining the results of using the SIDA passivity-based control method in wind system modeling under different weather conditions is crucial for determining the stability of internal parameter variations. The model of the DFIG and wind turbine includes several characteristics, which are presented in Table 1.

Table 1. DFIG	parameters u	used in	simul	lation	model
---------------	--------------	---------	-------	--------	-------

Parameter	Value	Unit	Wind turbine (WT)			
Pn	100	kW	R	35.25	m	
Rs	0.455	Ω	S	$\pi$ .r <sup>2</sup>	$m^2$	
Rr	0.19	Ω	ρ	1.22	$Kg/m^3$	
Ls	0.07	H	G	90	/	
Lr	0.0213	H	Jturbine	1000	$Kg/m^2$	
Lm	0.034	H				
JDFIG	0.53	Kg.m <sup>2</sup>				
f	0.0024	N.m.s/rad				
p	2	/				

In this context, Figures 7 to 9 illustrate the findings related to the durability of the SIDA-PBC method concerning its resilience to the influence of varying weather conditions and electrical loads (D-ZIP), while concurrently addressing changes in the internal resistance and inductance values of the DFIG. Figure 8 displays the outcomes concerning the resilience assessment of the SIDA-PBC approach in response to variations in the inductance value of the DFIG. The ensuing figure, denoted as Figure 9, encapsulates the obtained results pertaining to the SIDA-PBC technique's performance in terms of active and reactive power generation.

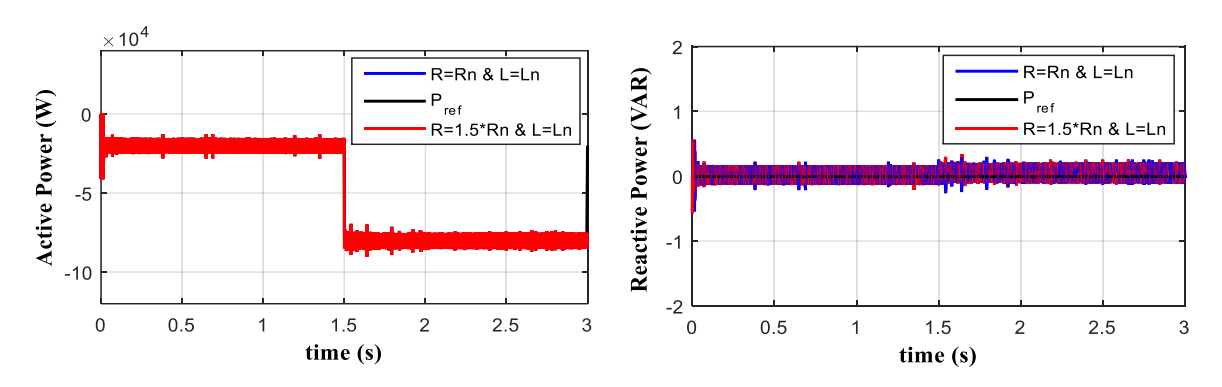


Figure 7. Effect of variations in internal resistances on the  $P_G$  and  $Q_G$  powers of the DFIG with SIDA-PBC

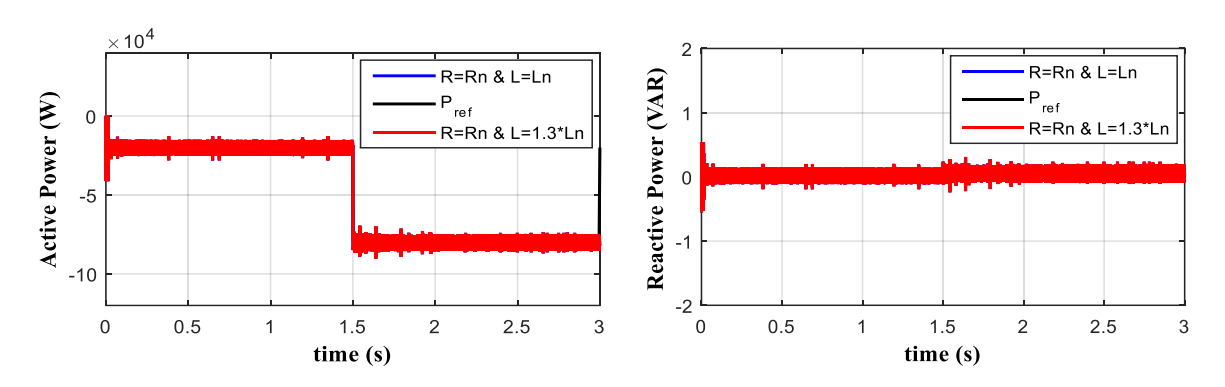


Figure 8. Effect of variations in internal inductance on the  $P_G$  and  $Q_G$  powers of the DFIG with SIDA-PBC

The provided content extensively discusses crucial aspects pertaining to the operational and stability aspects of the power grid at the integration point in Kabertene. The primary focus encompasses measures related to frequency and voltage control, the integration of renewable energy resources, and the efficacy of control methodologies. Illustrative figures, namely Figures 5 and 6, portray the efficacy of a frequency-tuning model designed to precisely rectify synchronization issues at the Kabertene integration point. The integration of the AFRR is revealed to exert a substantial positive impact on the overall system stability, effectively adhering to the stipulated frequency regulations mandated in Algeria. Notably, the infrastructure for electricity generation is engineered to endure rapid frequency fluctuations, ensuring seamless connection and synchronization, even in demanding circumstances. The regimen of frequency control strategies encompasses automatic voltage regulation and reactive power compensation, which collectively uphold voltage stability within permissible thresholds, thereby lending robust support to the dependable operation of the grid. Highlighting the influence of PV sources on voltage levels, Figure 5 captures temporal voltage

2210 ☐ ISSN: 2302-9285

deviations within the 220 KV and 30 KV systems. Furthermore, Figure 6 provides a visual representation of the highest voltage levels observed in the 220 KV and 30 KV buses, a parameter influenced by the interplay of frequency control strategies and the integration of renewable energy sources, including PV and wind. Table 1 and Figure 7 collaborate to furnish analytical insights into active loss reduction strategies. Rigorous data analysis guides these strategies, as the DFIG undergoes regulatory testing, culminating in interventions aimed at diminishing active losses and enhancing overall system efficiency.

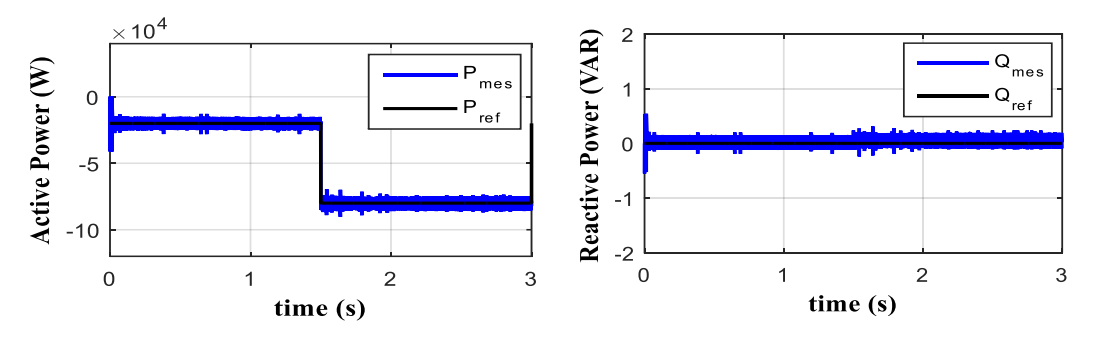


Figure 9.  $P_G$  and  $Q_G$  powers production regulation with SIDA-PBC method

The strategy draws on SIDA-PBC directives, aptly tracking reference trajectories during pursuit trials depicted in Figure 8. This approach effectively maintains power output within prescribed ranges, thereby averting persistent faults. The resilience of the system under fluctuating parameters is extensively examined through transient state durability assessments, vividly illustrated in Figures 8 and 9.

These evaluations vividly demonstrate the system's adaptability and unwavering performance, even when subjected to extreme parameter variations in dynamic conditions. Furthermore, the study introduces a state-feedback control strategy, adept at quelling disturbances, achieving convergence to reference trajectories, facilitating MPPT, and adeptly managing fluctuations in wind speed. This strategy emerges as a superior performer when navigating through challenging scenarios.

## 4. CONCLUSION

To summarize, the effective integration of Kabertene wind energy into the PIAT network involves implementing various control techniques for DFIGs. These techniques include passivity control, decentralized multivariable PID controllers, MPPT, frequency and voltage control, and PSO-based power optimization. These methods successfully address the challenges associated with integrating wind energy into the PIAT network.

These approaches enhance stability, reduce frequency and voltage variations, and ensure smooth integration of renewable energy. Applying PSO optimization to D-ZIP load profiles not only reduces active power losses, but also helps maintain voltage stability. The study provides practical insights into constructing a more environmentally friendly energy system. It highlights the impact of passivity-based control on active energy production and the importance of SIDA-PBC for Kabertene energy. Comparisons are concisely summarized. These findings provide valuable insights into the best way to incorporate renewable energy sources into the PIAT program. This will help in creating a sustainable energy landscape in Kabertene.

#### REFERENCES

- [1] H. Hichem, M. Abdellah, T. A. Abderrazak, B. Abdelkader, and S. Ramzi, "A wind turbine sensorless automatic control systems, analysis, modelling, and development of IDA-PBC method," *International Journal of Power Electronics and Drive Systems*, vol. 11, no. 1, pp. 45–55, 2020, doi: 10.11591/ijpeds.v11.i1.pp45-55.
- [2] T. A. Abderrazak, A. Iliace, B. M. Sofiane, B. R. Ilyas, H. Hichem, and C. Abdelkader, "Enhancing Frequency System Damping Efficiency via Optimal Integration of VRE in Grid," 2023 Second International Conference on Energy Transition and Security (ICETS), 2023, pp. 1-6, doi: 10.1109/ICETS60996.2023.10410747.
- [3] H. Wen, "Power flow analysis of 110kV power supply system based on PowerWorld," Journal of Physics: Conference Series, vol. 2495, no. 1, p. 012025, 2023, doi: 10.1088/1742-6596/2495/1/012025.
- [4] B. Kelkoul and Â. Boumediene, "Stability analysis and study between classical sliding mode control (SMC) and super twisting algorithm (STA) for doubly fed induction generator (DFIG) under wind turbine," *Energy*, vol. 214, no. 7, pp. 2776–2798, 2021, doi: 10.1016/j.energy.2020.118871.
- [5] T. A. Abderrazak, B. R. Ilyas, B. M. Sofiane, H. Hichem, and A. Iliace, "Advanced dynamic stability system developed for nonlinear load," *International Journal of Power Electronics and Drive Systems*, vol. 14, no. 4, pp. 2032–2043, 2023, doi:

П

- ISSN: 2302-9285
- 10.11591/ijpeds.v14.i4.pp2032-2043.
- [6] M. K. Kar, "Stability analysis of multi-machine system using FACTS devices," International Journal of System Assurance Engineering and Management, vol. 14, no. 6, pp. 2136–2145, 2023, doi: 10.1007/s13198-023-02044-6.
- [7] A. A. Tadjeddine, M. S. Bendelhoum, R. I. Bendjillali, H. Hamiani, and S. Djelaila, "VRE Integrating in PIAT grid with Optimal Techniques: A Case Study Kabertene," *EAI Endorsed Transactions on Energy Web*, vol. 10, 2023, doi: 10.4108/ew.3378.
- [8] K. E. Okedu and H. F. A. Barghash, "Enhancing the performance of DFIG wind turbines considering excitation parameters of the insulated gate bipolar transistors and a new PLL scheme," Frontiers in Energy Research, vol. 8, no. 7, pp. 2776–2798, 2021, doi: 10.3389/fenrg.2020.620277.
- [9] H. R. Karimi, "Structural control and fault detection of wind turbine systems," Structural Control and Fault Detection of Wind Turbine Systems, pp. 1–302, 2018, doi: 10.1049/pbp0117e.
- [10] A. Tadjeddine, M. Bendelhoum, I. Arbaoui, R. Bendjillali, and M. Alami, "Optimizing Frequency Stability in Distributed Power Grids through Advanced Power Flow Control with 25MW Photovoltaic Integration," *Advances in Systems Science and Applications*, vol. 23, no. 4, pp. 18-30, Dec. 2023.
- [11] Z. Chai, H. Li, X. Xie, M. Abdeen, T. Yang, and K. Wang, "Output impedance modeling and grid-connected stability study of virtual synchronous control-based doubly-fed induction generator wind turbines in weak grids," *International Journal of Electrical Power and Energy Systems*, vol. 126, 2021, doi: 10.1016/j.ijepes.2020.106601.
- [12] S. Mensou, A. Essadki, I. Minka, T. Nasser, B. B. Idrissi, and L. B. Tarla, "Performance of a vector control for dfig driven by wind turbine: Real time simulation using DS1104 controller board," *International Journal of Power Electronics and Drive Systems*, vol. 10, no. 2, pp. 1003–1013, 2019, doi: 10.11591/ijpeds.v10.i2.pp1003-1013.
- [13] H. Chojaa *et al.*, "Advanced control techniques for doubly-fed induction generators based wind energy conversion systems," in *IEEE Global Energy Conference*, IEEE, 2022, pp. 282–287, doi: 10.1109/GEC55014.2022.9987088.
- [14] A. D. Falehi and H. Torkaman, "Promoted supercapacitor control scheme based on robust fractional-order super-twisting sliding mode control for dynamic voltage restorer to enhance FRT and PQ capabilities of DFIG-based wind turbine," *Journal of Energy Storage*, vol. 42, 2021, doi: 10.1016/j.est.2021.102983.
- [15] X. Lyu, Y. Jia, Z. Xu, and X. Xu, "An active power regulation strategy for wind farm considering wake effect," 2019 IEEE Power & amp; Energy Society Innovative Smart Grid Technologies Conference (ISGT), Feb. 2019, doi:10.1109/isgt.2019.8791662.
- [16] H. Hamiani, A. A. Tadjeddine, M. Sekkal, and I. Arbaoui, "Non-linear control by status feedback of the three-phase asynchronous machine," *Algerian Journal of Renewable Energy and Sustainable Development*, vol. 5, no. 1, pp. 1–10, 2023, doi: 10.46657/ajresd.2023.5.1.1.
- [17] H. Chojaa *et al.*, "Enhancement of direct power control by using artificial neural network for a doubly fed induction generator-based WECS: an experimental validation," *Electronics (Switzerland)*, vol. 11, no. 24, p. 4106, 2022, doi: 10.3390/electronics11244106.
- [18] A. A. Tadjeddine, I. Arbaoui, A. Harrouz, H. Hamiani, and C. Benoudjafer, "Dispatching and scheduling at load peak with the optimal location of the compensation under constraints in real-time," *Algerian Journal of Renewable Energy and Sustainable Development*, vol. 2, no. 01, pp. 34–41, 2020, doi: 10.46657/ajresd.2020.2.1.5.
- [19] H. Huerta, A. G. Loukianov, and J. M. Canedo, "Passivity sliding mode control of large-scale power systems," *IEEE Transactions on Control Systems Technology*, vol. 27, no. 3, pp. 1219–1227, 2019, doi: 10.1109/TCST.2018.2791928.
- [20] A. H. Sun H, "Passivity-based slidingmode control for input-affine nonlinear systems," *Paper presented at: 2016 American Control Conference*, 2016.
- [21] R. Prasad and N. P. Padhy, "Active Power Dispatch and tracking mechanism for DFIG wind turbine generator in wind farm considering wake effect," 2022 IEEE International Conference on Power Electronics, Smart Grid, and Renewable Energy (PESGRE), Jan. 2022, doi:10.1109/pesgre52268.2022.9715911.
- [22] S. Tamaro and C. L. Bottasso, "A new wind farm active power control strategy to boost tracking margins in high-demand scenarios," 2023 American Control Conference (ACC), May 2023, doi:10.23919/acc55779.2023.10156275.
- [23] R. A. Othman and O. S. Alyozbaky, "A Novel Method to Improve the Power Quality Via Hybrid System," Przeglad Elektrotechniczny, vol. 2023, no. 6, pp. 167–174, Jun. 2023, doi: 10.15199/48.2023.06.35.
- [24] A. A. Tadjeddine, A. Chaker, M. Khiat, L. Abdelmalek, and N. Khalfalah, "A contribution to the control of voltage and power of the interconnection between two decentralized electrical grids with an optimal localization of the SVC devices in real-time," International Journal of Power Electronics and Drive Systems, vol. 10, no. 1, pp. 170–177, 2019, doi: 10.11591/ijpeds.v10.i1.pp170-177.
- [25] A. Tadjeddine Ali, I. Arbaoui, H. Hamiani, and A. Chaker, "Optimal distribution of power under stress on power grid in real-time by reactive compensation-management and development in balance," *International Journal of Power Electronics and Drive Systems*, vol. 11, no. 2, pp. 685–691, 2020, doi: 10.11591/ijpeds.v11.i2.pp685-691.
- [26] W. Li et al., "A wind farm active power dispatch strategy considering the wind turbine power-tracking characteristic via model predictive control," Processes, vol. 7, no. 8, p. 530, Aug. 2019, doi:10.3390/pr7080530.
- [27] L. Bena, M. Nowak, and M. Kusinski, "Analysis of the impact of micro photovoltaic installations on the voltage in the low voltage distribution network," in *Selected Issues of Electrical Engineering and Electronics*, IEEE, 2021, pp. 1–6, doi: 10.1109/WZEE54157.2021.9577036.
- [28] M. Nowak, T. Binkowski, and S. Piróg, "Proportional-resonant controller structure with finite gain for three-phase grid-tied converters," *Energies*, vol. 14, no. 20, p. 6726, 2021, doi: 10.3390/en14206726.
- [29] Z. Mahmoudi, E. Darbanian, and M. Nickray, "Optimal energy consumption and cost performance solution with delay constraints on fog computing," *Jordanian Journal of Computers and Information Technology*, vol. 9, no. 2, pp. 76–93, 2023, doi: 10.5455/jjcit.71-1667637331.
- [30] B. T. Karim, A. Allali, H. M. Boulouiha, and M. Denai, "Voltage profile and power quality improvement using multicell dynamic voltage restorer," *International Journal of Power Electronics and Drive Systems*, vol. 13, no. 4, pp. 2216–2225, 2022, doi: 10.11591/ijpeds.v13.i4.pp2216-2225.
- [31] I. Arbaoui, A. Hamou, A. Tadjeddine, A. Harrouz, and C. Benoudjafer, "Acoustic study of noise generated by arzew's industrial units in limited batteries," *Algerian Journal of Renewable Energy and Sustainable Development*, vol. 2, no. 02, pp. 115–125, 2020, doi: 10.46657/ajresd.2020.2.2.4.
- [32] M. Mattioni, S. Monaco, and D. Normand-Cyrot, "IDA-PBC for LTI dynamics under input delays: a reduction approach," in Proceedings of the American Control Conference, IEEE, 2021, pp. 2497–2502, doi: 10.23919/ACC50511.2021.9482818.

#### **BIOGRAPHIES OF AUTHORS**



Tadjeddine Ali Abderrazak is an instructor in the Electrical Engineering Department at the University Nour Bachir, located in El-Bayadh, Algeria. He possesses both a master's and a Ph.D. in Electrical Engineering from the National Polytechnic School of Oran (ENPO-MA, Oran-Algeria). His main research interests cover a wide range of topics in power systems engineering, such as electrical power engineering, power systems analysis, power transmission, voltage regulation, and electrical energy conservation, optimization in distribution systems, energy conversion, and renewable energy. He has authored or coauthored more than 100 research publications, demonstrating his active involvement in developing knowledge in various domains. He can be contacted at email: atadj1@gmail.com.



**Arbaoui Iliace** si san Associate Professor at the Department of Electrical Engineering, Adrar University-Algeria. He received a master's and a Ph.D. degree in physic at University Oran, Ahmed ben Bella, Algeria. He is a professor at Adrar University, Algeria. His research activities include physic's problems and renewable energy. He can be contacted at email: arbaoui.iliace@gmail.com.





Bendelhoum Mohammed Sofiane below sofiane below systems from Tlemcen University, Algeria. He also received his Ph.D. from Sidi Bel Abbes University, Algeria. Since 2014, he has been an Associate Professor at the University of El-Bayadh and performs his research at the Instrumentation Laboratory and Advanced Materials University Center. His research interests are primarily in the area of image processing, medical image compression, wavelets transform turbo-encoding, turbo equalization, wireless communications, and networks as well as biomedical engineering, where he is the author/co-author of over 65 research publications. He can be contacted at email: bendelhoum med@yahoo.fr.



Bendjillali Ridha Ilyas was born in Bechar, Algeria. He received a Master degree in Digital Communication Systems from Tahri Mohammed University of Bechar, Algeria, in 2016, and a Ph.D. degree in Information Processing and Telecommunications at Tahri Mohammed University of Bechar, Algeria, in 2020. His main research areas are image and video processing, pattern recognition, computer vision, and machine learning. He can be contacted at email: rayben43@gmail.com.